nature synthesis

ARTICLES

https://doi.org/10.1038/s44160-022-00024-5

Check for updates

Iron-catalysed reductive cross-coupling of glycosyl radicals for the stereoselective synthesis of C-glycosides

Quanquan Wang[1,5], Qikai Sun[2,5], Yi Jiang[1], Huixing Zhang[2], Lu Yu[3], Changlin Tian[3,4], Gong Chen[2,6] ✉ and Ming Joo Koh[1,6] ✉

Stereochemically defined C-glycosides are prized for their biological activity. Developing a catalytic method that comprises non-precious metals to synthesize these C-glycosides remains challenging. Here, starting from readily accessible glycosyl chlorides, we show that an Earth-abundant iron-based catalyst promotes the facile generation of glycosyl radicals, which either react directly with an unsaturated electrophile or are captured by an organonickel species to facilitate C–C bond formation under mild reductive conditions. Exploration of these two reaction pathways across a range of substrates has produced a diverse array of C-glycoside products functionalized with alkenyl, alkynyl or aromatic anomeric groups, with excellent diastereocontrol. Mechanistic control and electron paramagnetic resonance spectroscopic experiments indicate that the active catalytic species is a low-valent iron complex formed through Mn reduction. The method was applied in the stereoselective synthesis of bioactive C-glycosides and therapeutically relevant analogues.

Since its advent, transition metal-catalysed cross-coupling has revolutionized the art of chemical synthesis[1–4]. By offering a direct avenue for the union of two or more entities to generate molecular complexity, the field has far-ranging applications across academia and industry[5]. In recent years, the renaissance of non-precious base metal catalysis[6–8] has stimulated remarkable developments in cross-coupling by enabling a broader set of organic precursors to be merged to access new chemical space that is often unattainable by noble-metal-based catalysts[9,10]. In particular, the use of catalysts derived from non-toxic iron, the most abundant and inexpensive transition metal in the Earth's crust[11–13], is naturally appealing to chemists for economic and environmental reasons. Although iron-catalysed cross-coupling[14,15] has seen substantial progress in recent years, the developments in this area and its utility in organic synthesis are still pale in comparison with those of the more established transition metals, such as palladium[16]. This owes, in part, to iron's ability to adopt a large number of oxidation states and spin states[17,18], which consequently elevates the difficulty of manipulating organoiron chemistry to facilitate C–C bond formation. However, iron-catalysed reactions between two bench-stable electrophilic substrates[19], which would effectively eliminate the requirement for unstable and basic organometallic reagents[20], are scarce and underdeveloped.

In light of the aforementioned challenges, it is unsurprising that iron catalysis is rarely employed in the context of complex C-glycoside synthesis[21–27]. Stereochemically pure glycosides with a functionalized alkenyl, alkynyl or heteroaryl substituent on the anomeric carbon play vital roles in various studies that pertain to biological functions[28,29] and diseases[30] (Fig. 1a). These motifs are embedded within the frameworks of countless therapeutically active compounds[31,32], which renders them attractive candidates for further development in drug discovery programmes[33]. In the past decade, only a handful of iron-catalysed syntheses that deliver C-glycosides have been disclosed. In one instance, the union of glycosyl halides with presynthesized aryl(alkenyl)zinc compounds was carried out at a reduced temperature in the presence of an iron complex that bore a sizeable and sophisticated bisphosphine ligand (Fig. 1b[25]). Other cases relied on reactions of the Michael–Giese type to combine glycals with activated alkenes in the presence of excess hydrosilane to afford a limited range of C-alkyl glycosides (Fig. 1c (ref. [26] and 1d (ref. [27]).

Based on the reportedly high reactivity of iron species towards alkyl halides[34–39], we wondered if we could identify an appropriate iron-based complex, in conjunction with an inexpensive reducing agent[40], to induce the formation of a glycosyl radical[41] species from readily available and bench-stable glycosyl chloride donors **4** through a Cl atom abstraction[32,41] to give a radical cage pair[42,43] **i** (Fig. 2a). After cage escape, the glycosyl radical could directly react with a sp^2- or sp-hybridized organohalide or pseudohalide **5** through an iron-mediated stereocontrolled radical addition/β-halide elimination[19,44] to furnish **6** in high diastereoselectivity via **ii**. Alternatively, the incorporation of a suitable nickel-based co-catalyst[45] that first activates **5** to generate an organonickel intermediate **iii**, followed by stereocontrolled association with the glycosyl radical (to give **iv**) and reductive elimination would also afford **6**. By implementing this two-pronged approach, sensitive organometallic reagents can be avoided and access to a diverse assortment of glycosides that bear C–C(sp^2/sp) glycosidic bonds can be accomplished.

Although nickel-catalysed reductive[46] as well as metallaphotoredox-catalysed[45,47,48] protocols have been separately

[1]Department of Chemistry, National University of Singapore, Singapore, Republic of Singapore. [2]State Key Laboratory and Institute of Elemento-Organic Chemistry, College of Chemistry, Nankai University, Tianjin, China. [3]High Magnetic Field Laboratory, Chinese Academy of Sciences, Hefei, China. [4]Hefei National Laboratory for Physical Sciences at the Microscale and School of Life Sciences, University of Science and Technology of China, Hefei, China. [5]These authors contributed equally: Quanquan Wang, Qikai Sun. [6]These authors jointly supervised this work: Gong Chen & Ming Joo Koh. ✉e-mail: gongchen@nankai.edu.cn; chmkmj@nus.edu.sg

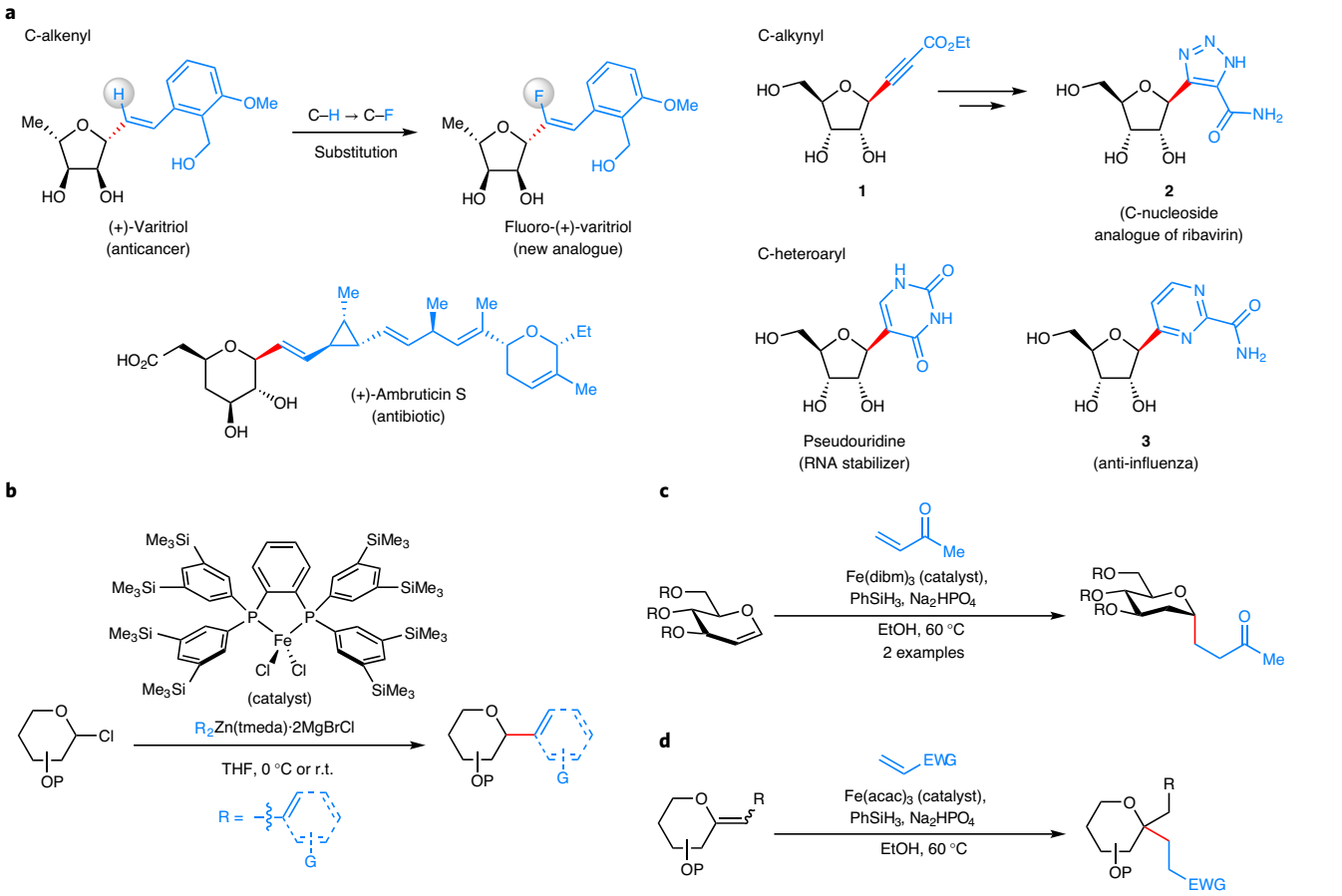

Fig. 1 | The significance of C-glycosides and the existing iron-catalysed protocols that generate them. a, Examples of C–R (R = alkenyl, alkynyl or heteroaryl) glycoside motifs in naturally occurring and synthetic bioactive compounds. **b**, Iron-catalysed methods that deliver C-glycosides are scarce and limited in scope. For instance, the cross-coupling of glycosyl halides and organozinc reagents requires an iron(II) catalyst that bears a sizeable bisphosphine ligand at a low temperature. **c**,**d**, Fe(III) complexes can mediate Michael–Giese-type reactions of glycals and electron-deficient olefins in the presence of excess hydrosilane, but a syringe pump addition of the olefin and/or hydrosilane is sometimes necessary to improve yields. R, G, functional groups; P, protecting group; EWG, electron-withdrawing group; acac, acetylacetonate; dibm, diisobutyrylmethane; tmeda, tetramethylethylenediamine; r.t., room temperature.

devised to generate C-heteroaryl(aryl) and/or C-alkenyl glycosides, enduring shortcomings remain: (1) Alkenyl- and heteroaryl-substituted cross-coupling partners usually involve iodides or bromides, and reactions with the more abundant[49] but less reactive chlorides or fluorides are scarce. Furthermore, there are no examples with pseudohalides, such as triflates, which can be derived from readily available phenols and ketones[50–52]. (2) For catalytic reactions that give C-alkenyl glycosides, the formation of fluorinated analogues (for example, fluoro-varitriol in Fig. 1a) have not been documented[46,53–55]. Such products are highly valuable, given that olefinic C–H → C–F bond substitution[56] often imparts desirable biological attributes such as enhanced potency, metabolic stability and bioavailability to the parent molecule[57]. (3) Catalytic processes that install highly Lewis basic heterocycles on the anomeric carbon are sometimes inefficient[45,46]. Access to these C-heteroaryl glycosides, which form the core of medicinally relevant C-nucleoside derivatives[28,30,58], is often thwarted by catalyst deactivation[59] as a result of the competitive heteroarene coordination to the metal centre. (4) Limited examples of reactions that lead to C-alkynyl glycosides[60,61], which are useful precursors to glycosyl triazoles[62], have been demonstrated. Here we describe a versatile reductive cross-coupling strategy using base metal catalysis that addresses these challenges to deliver various classes of C–R (R = alkenyl, alkynyl, aryl, heteroaryl) glycosides in high efficiency and stereoselectivity (Fig. 2b).

Results

Reaction optimization and mechanistic evaluation. D-Mannofuranosyl chloride **4a** was chosen as the glycosyl donor to evaluate the conditions for cross-coupling with different organohalides (Fig. 3). After examining various transition metal salts, ligands, reducing agents and solvents (Supplementary Tables 1–7), we found that ligand-free $FeBr_2$ was optimal in promoting reductive cross-coupling with *E*-alkenyl halides **5a–5c** in the presence of manganese as reductant and THF as solvent to deliver the desired C-alkenyl glycoside α-**6a** in 65–80% yields and full stereoretention of the starting haloalkene geometry. Other Fe(II) and Fe(II) salts were inferior, and the addition of ligands was detrimental to the efficiency (Supplementary Table 2). Given that simple iron salts are typically incapable of inducing oxidative cleavage of C(sp^2)–Cl bonds[63], and that fluoroalkenes also serve as effective reagents under the reaction conditions (see Table 1 for details), we surmised that the Fe-catalysed alkenylation probably proceeds through an addition–elimination pathway[19]. Control experiments further revealed that the C-alkenyl glycoside product was generated as a single *E* isomer regardless of the stereochemistry of the haloalkene used (see Supplementary Fig. 20 for details), which means that the reagent does not need to be isomerically pure. In contrast, the reaction between **4a** and heteroaryl chloride **5d** required a co-catalyst derived from $NiBr_2$·diglyme/**L1** (Table 1) in addition to $FeBr_2$

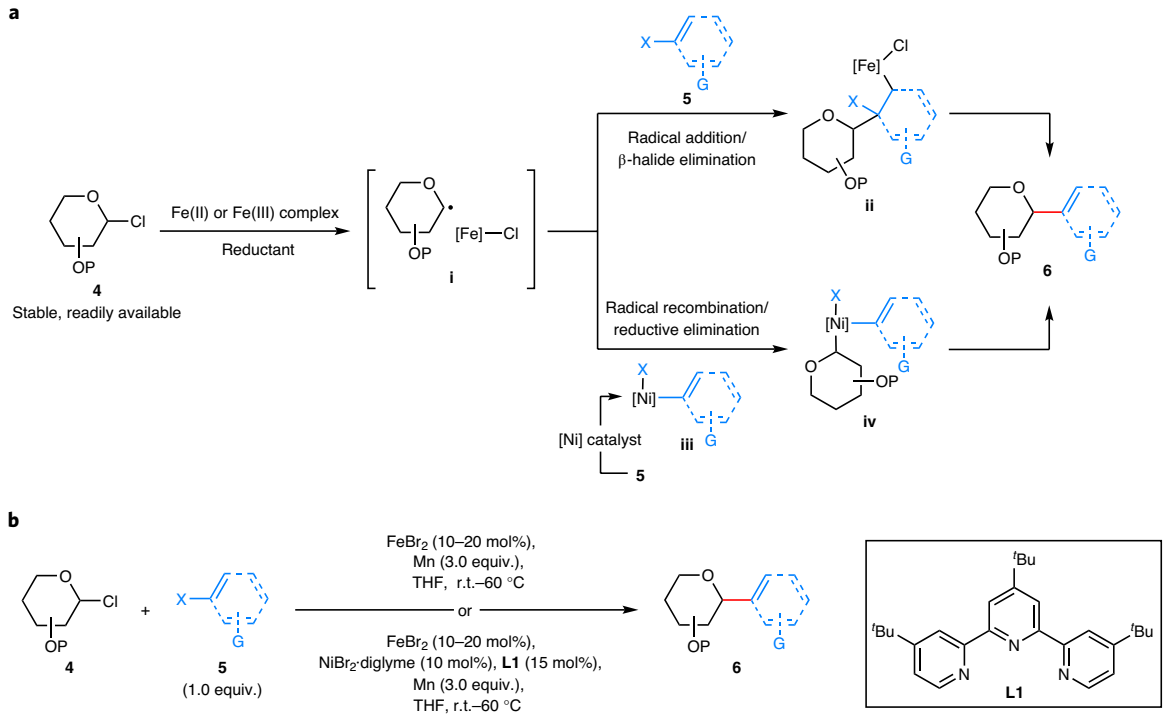

Fig. 2 | Designing a reductive strategy that leverages iron catalysis to access diverse stereodefined C-glycosides. a, Stereoselective synthesis of C-glycosides by a two-pronged approach in cross-electrophile coupling via radical intermediates obtained from the iron-catalysed activation of readily accessible glycosyl chlorides. **b**, The single Fe or dual Fe–Ni manifold offers access to products with C–C(sp^2/sp) glycosidic bonds in high efficiency and anomeric selectivity. G, functional group; P, protecting group; X, halide or pseudohalide; L, ligand; diglyme, diethylene glycol dimethyl ether.

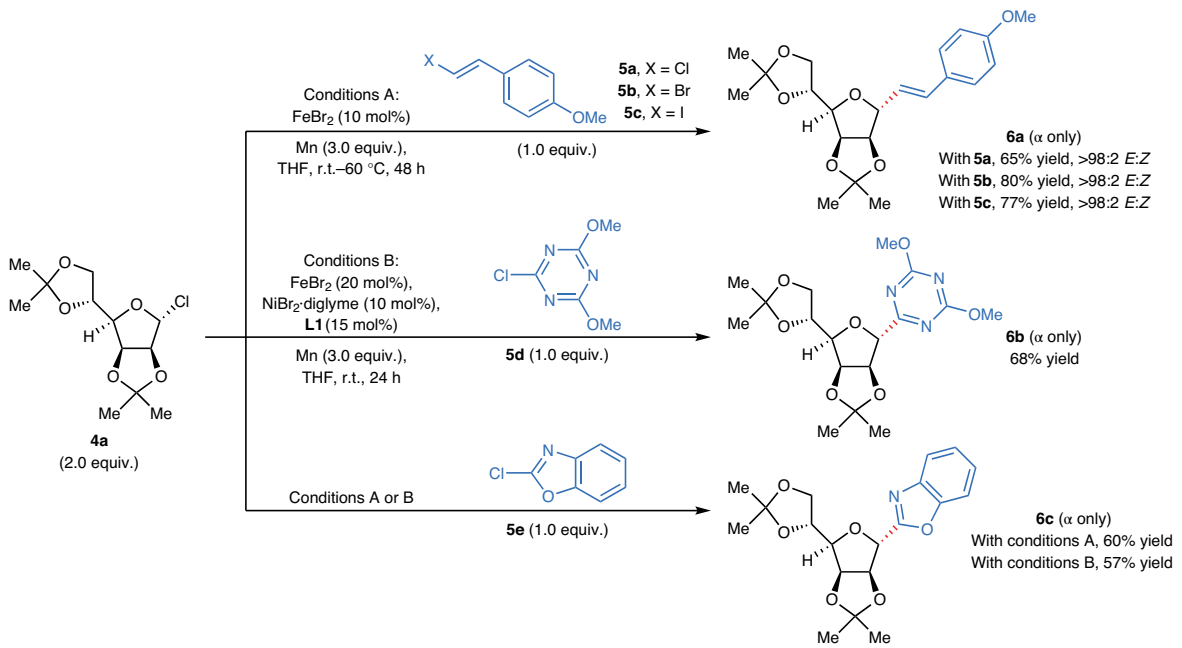

Fig. 3 | Reaction development. Examination of the reaction conditions for cross-electrophile coupling with Fe or Fe–Ni catalysis. For the synthesis of C-heteroaryl glycoside **6b**, a dual Fe–Ni catalytic regime is required. Only trace amounts of the product were detected using either the Fe or Ni complex alone. The α:β anomeric ratios and *E*:*Z* ratios were determined by gas chromatography and ^{1}H NMR analysis. Yields are for isolated and purified products.

to promote C–C bond formation, affording **6b** in 68% yield as a single α-anomer. Intriguingly, the reactivity was poor in the presence of either the Fe or Ni complex alone (Supplementary Table 8). We speculated that glycosyl radical formation could be less facile with $NiBr_2$·diglyme (versus that with $FeBr_2$), whereas **5d** might be incompetent in undergoing glycosyl radical addition–elimination[64], which necessitates the addition of a Ni co-catalyst for activation (see Fig. 4 for more details). Notably, <2% conversion to **6b** was

Table 1 | Stereoselective synthesis of C-alkenyl and C-alkynyl glycosides

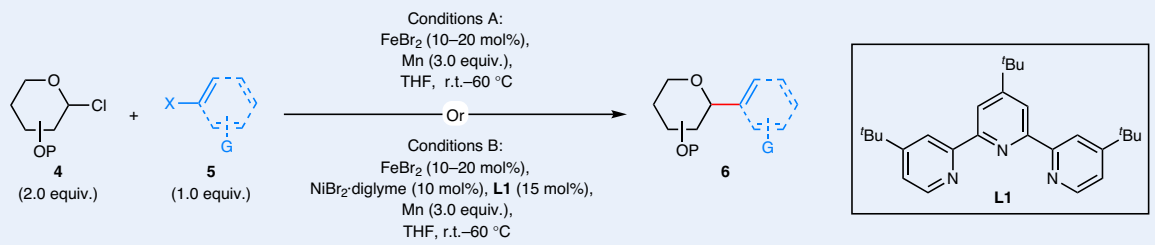

D-mannofuranose

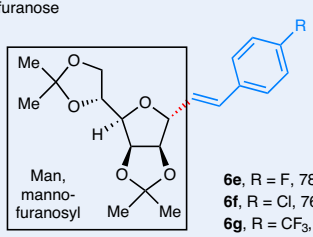

6e, R = F, 78% yield, α, >98:2 *E*:*Z*
6f, R = Cl, 76% yield, α, >98:2 *E*:*Z*
6g, R = CF_3, 73% yield, α, >98:2 *E*:*Z*

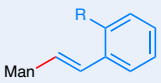

6h, R = Me, 61% yield, α, >98:2 *E*:*Z*
6i, R = OMe, 75% yield, α, >98:2 *E*:*Z*

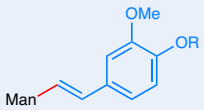

6j, R = Bn, 66% yield, α, >98:2 *E*:*Z*
6k, R = TBS, 60% yield, α, >98:2 *E*:*Z*

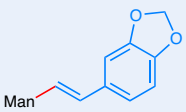

6l
82% yield, α, >98:2 *E*:*Z*

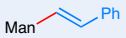

6m
64% yield, α, >98:2 *E*:*Z*

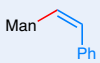

6n[a]
74% yield, 6.6:1 α:β, >98:2 *Z*:*E*

6o
51% yield, α, >98:2 *E*:*Z*

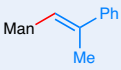

6p
54% yield, α, >98:2 *E*:*Z*

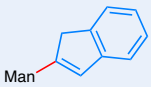

6q[b]
49% yield, α

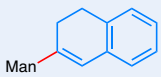

6r[c]
38% yield (56% yield[a]), α

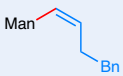

6s[a,d]
57% yield, α, >98:2 *Z*:*E*

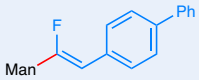

6t[e]
62% yield, α, >98:2 *Z*:*E*

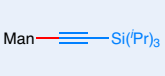

6u[d]
61% yield, α

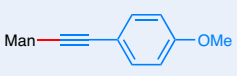

6v[d]
41% yield, α

D-mannopyranose

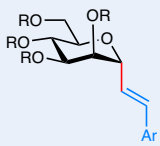

6w, R = Bn, Ar = 4-OMe-C_6H_4,
71% yield, α, >98:2 *E*:*Z*
6x, R = Bn, Ar = 4-Cl-C_6H_4,
64% yield, α, >98:2 *E*:*Z*
6y, R = Me, Ar = 4-OMe-C_6H_4,
48% yield, α, >98:2 *E*:*Z*

D-galactopyranose

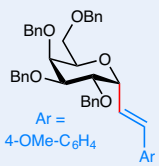

6z
43% yield (57% yield[d]), α, >98:2 *E*:*Z*

L-rhamnopyranose

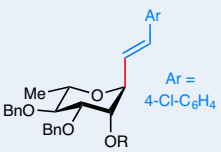

6aa, R = Bn, 69% yield, α, >98:2 *E*:*Z*
6ab, R = Ac, 81% yield, 12:1 α:β, >98:2 *E*:*Z*

D-arabinofuranose

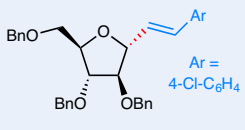

6ac[f]
80% yield, α, >98:2 *E*:*Z*

D-ribofuranose

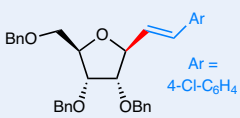

6ad
41% yield, β, >98:2 *E*:*Z*

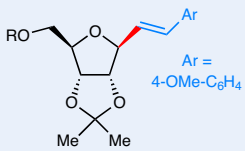

6ae, R = Bz, 60% yield, 1:7.3 α:β, >98:2 *E*:*Z*
6af, R = TBDPS, 70% yield, 1:7 α:β, >98:2 *E*:*Z*

D-lyxofuranose

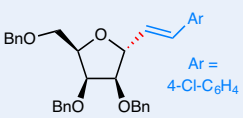

6ag
61% yield, α, >98:2 *E*:*Z*

D-gulofuranose

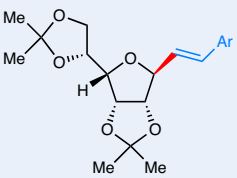

6ah, Ar = 4-OMe-C_6H_4,
77% yield, β, >98:2 *E*:*Z*
6ai, Ar = 4-Cl-C_6H_4,
71% yield, β, >98:2 *E*:*Z*

Unless otherwise stated, all the reactions were conducted using conditions A with organobromides (X = Br). The α:β anomeric ratios and *E*:*Z* ratios were determined by ^{1}H NMR analysis. Yields are for the isolated and purified products. [a]Conditions B were used. [b]Glycosyl donor **4** (3 equiv.) and Mn (5 equiv.) were used. [c]Organotriflate was used. [d]Organoiodide was used. [e]1,1-Difluoroalkene was used. [f]Glycosyl donor **4** (3 equiv.) was used. TBDPS, *tert*-butyldiphenylsilyl.

observed under previously disclosed Ni-catalysed conditions[46]. However, cross-coupling with 2-chlorobenzoxazole **5e** was found to be similarly efficient using the single Fe (conditions A (Methods)) or dual Fe–Ni (conditions B (Methods)) regime to furnish α-*E*-**6c** in ~60% yield.

Additional experiments were performed to acquire more insights. As shown in Fig. 4a, exposing **4a** to 10 mol% $FeBr_2$ and Mn at ambient temperature in the absence of the cross-coupling partner led to a mixture of primarily hydrodechlorinated product **7** (22%) and diastereomeric radical homocoupling product **8** (13%). This suggests that glycosyl chlorides are effective precursors of radical intermediates, which are susceptible to homocoupling[65] or reaction with trace moisture[66] (reaction in d_8-THF as the solvent showed that THF was not the hydrogen donor). Further control reactions and electron paramagnetic resonance studies revealed that the species responsible for activating **4a** to generate the glycosyl radical is likely to be a low-valent iron complex obtained in situ by Mn reduction (see Supplementary Sections 6.7–6.9 for details). On the contrary, there was only 11% conversion to **7** in the presence of $NiBr_2$·diglyme under otherwise similar conditions, which may account for the lack of reactivity between **4a** and **5d** when $FeBr_2$ was excluded (Fig. 3). To probe the fate of the glycosyl radical in the presence

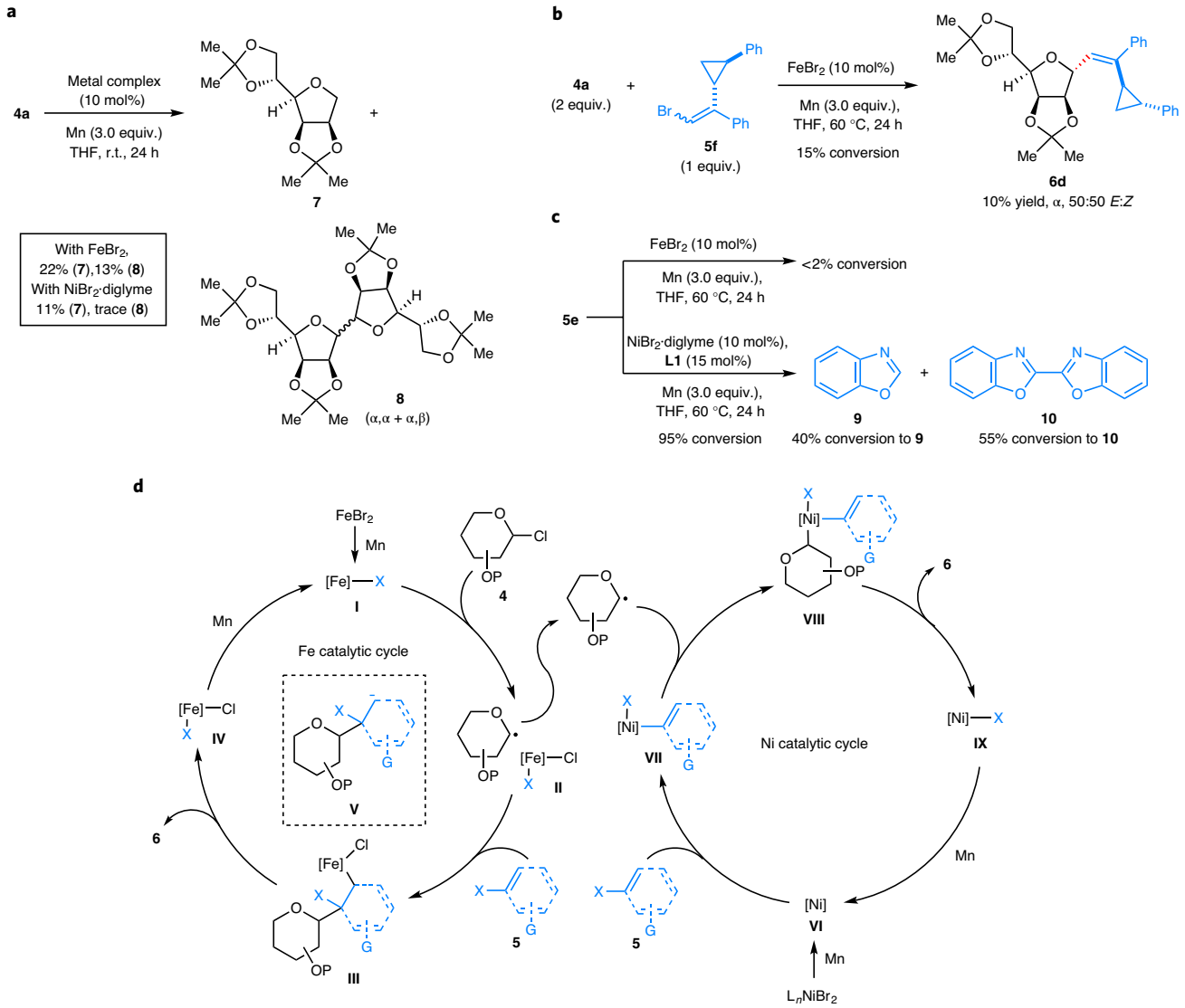

Fig. 4 | Mechanistic studies. a, Fe catalysis was found to promote more efficient glycosyl radical formation compared with that of Ni catalysis in the control experiments with **4a**. Yields of **7** and **8** are based on gas chromatography analysis. **b**, A radical clock experiment with **5f** suggests that the formation of any long-lived radical species is unlikely in the reaction system. **c**, Reactions with **5e** show that the Fe-catalysed reaction follows a distinct mechanism that probably does not involve oxidative addition–reductive elimination. **d**, Proposed catalytic mechanism for cross-electrophile coupling to generate C-glycosides. Mn reduction of $FeBr_2$ generates **I**, which activates **4** to generate **II**. Direct cross-coupling of the glycosyl radical with **5** by Fe-induced selective addition/β-halide elimination via **III** or **V** affords **6** and **IV**, which is reconverted into **I** by Mn reduction. Alternatively, in the Fe–Ni dual catalytic system, a concurrent nickel catalytic cycle that involves the oxidative addition of **VI** with **5** generates **VII**, which selectively captures the glycosyl radical to form **VIII**. Reductive elimination then releases **6** and **IX**, which is reduced back to **VI** by Mn. Conversions, α:β anomeric ratios and *E*:*Z* ratios were determined by gas chromatography and ^{1}H NMR analysis. Yields are for isolated and purified products, unless otherwise stated. L_n, ligands.

of an alkenyl halide, we conducted the Fe-catalysed cross-coupling using bromoalkenylcyclopropane **5f**, previously reported to serve as a radical clock substrate[67]. In the event (Fig. 4b), α-**6d** was obtained in 10% yield (50:50 *E*:*Z* ratio) with <2% ring rupture, which intimates that a glycosyl radical addition to the C=C bond to afford a transient benzylic radical species is less likely[68]. Instead, radical addition may be synchronous with C–Fe bond formation[19] prior to β-halide elimination.

To establish the dichotomy in reactivity modes between the single Fe and dual Fe–Ni catalytic manifolds, **5e** was separately subjected to $FeBr_2$ and $NiBr_2$·diglyme/**L1** in the presence of Mn without any glycosyl chloride (Fig. 4c). Unsurprisingly, there was <2% conversion using $FeBr_2$, and 95% conversion to reduction[69] and homocoupling[70] products **9** and **10** with the Ni system. These results substantiate the plausible involvement of a nickel catalytic cycle (under conditions B) that follows an oxidative addition/reductive elimination mechanism, whereas a direct iron-mediated glycosyl radical addition/β-halide elimination[64] pathway was responsible for the generation of **6c** under conditions A. On the basis of our experimental observations, a tentative catalytic pathway is illustrated in Fig. 4d. In the presence of Mn, the reduction of $FeBr_2$ probably occurs to form a low-valent iron species[37] **I** (Mn is oxidized to Mn(II) simultaneously), which triggers chlorine atom abstraction from **1** to afford the radical cage pair **II**. With a suitable unsaturated electrophile **5** (for example, alkenyl halide **5a**), the putative glycosyl radical (stabilized by anomeric effects[41,46]) undergoes regio- and diastereoselective addition (from the sterically less-hindered face) across the carbon–carbon π-bond to generate organoiron complex

Table 2 | Stereoselective synthesis of C-heteroaryl(aryl) glycosides

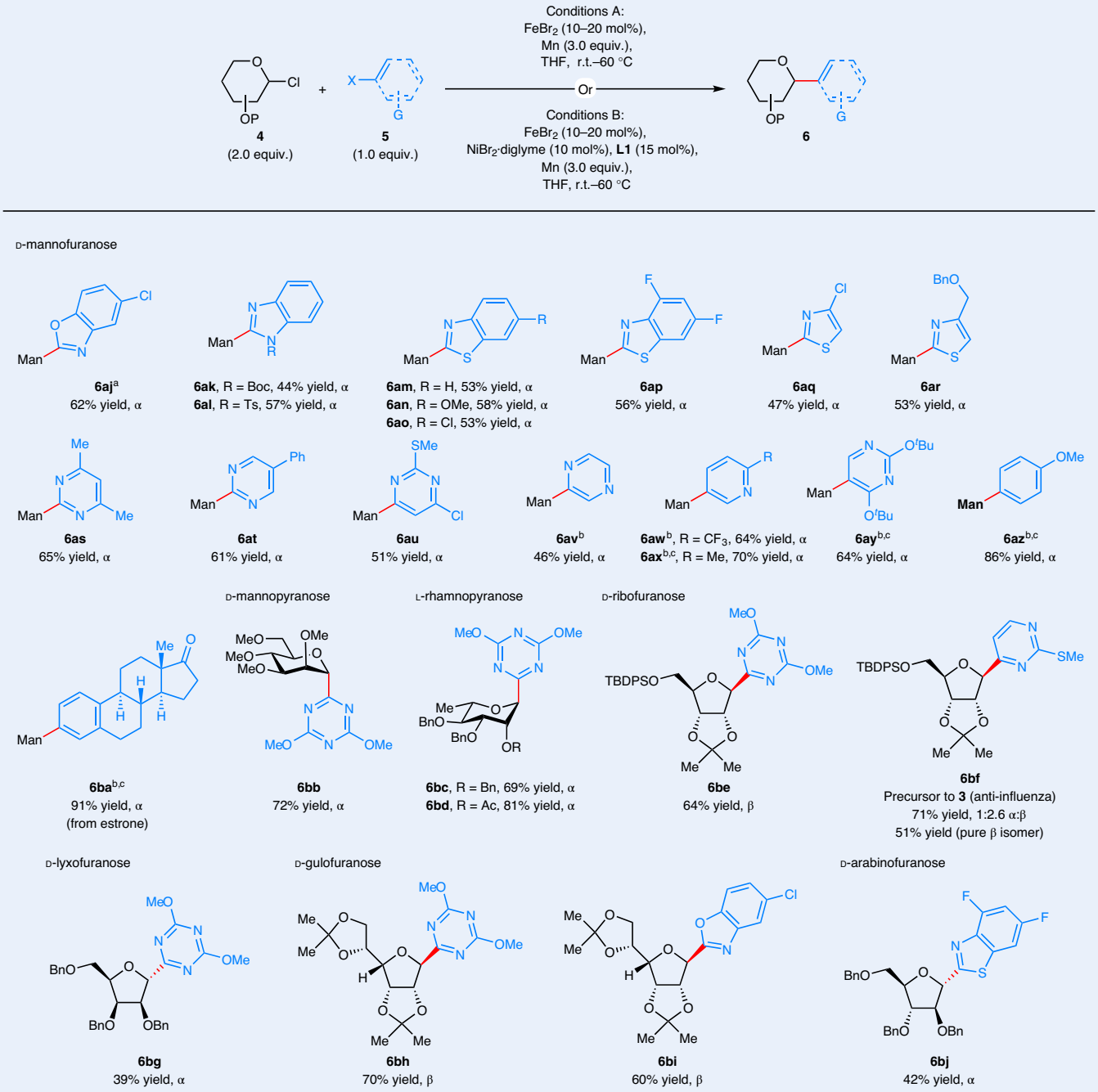

Unless otherwise stated, all the reactions were conducted using conditions B with organochlorides (X = Cl). The α:β anomeric ratios and *E*:*Z* ratios were determined by ^{1}H NMR analysis. Yields are for isolated and purified products. [a]Conditions A were used. [b]*N*,*N*-dimethylacetamide was used as the solvent. [c]Organotriflate was used.

III. At this juncture, a concerted 1,2-elimination[44] to regenerate the C=C bond and release the C-glycoside product **6** in high anomeric selectivity is concomitant with the formation of iron halide **IV**. Alternatively, the reduction of **III** by Mn (ref. [19]) to deliver a resonance-stabilized carbanion[67] intermediate **V** cannot be ruled out. When **5** is a haloalkene, the conformational flexibility of **V** possibly allows for a C–C bond rotation before the halide elimination[19] to give **6**, which may account for the stereoconvergent nature of the reaction using isomeric alkenyl halides (Supplementary Fig. 20).

For certain electrophiles (for example, heteroaryl halide **5d**), successful C–C bond formation relies on the involvement of a concurrent nickel catalytic cycle. Oxidative insertion of the active nickel complex **VI** (from Mn reduction) with **5** generates organonickel intermediate **VII**, which diastereoselectively associates with the glycosyl radical species from **II** (via a transition state stabilized by the donation of electron density on the ring oxygen to the antibonding orbital of the newly generated C–Ni bond)[45,46] to afford glycosylnickel **VIII**, which is expected to adopt a conformation stabilized by metallo-anomeric effects[71]. After a stereoretentive reductive elimination, the desired product **6** is obtained. Finally, a single-electron reduction of **IX** back to **VI** occurs to turn over the cycle.

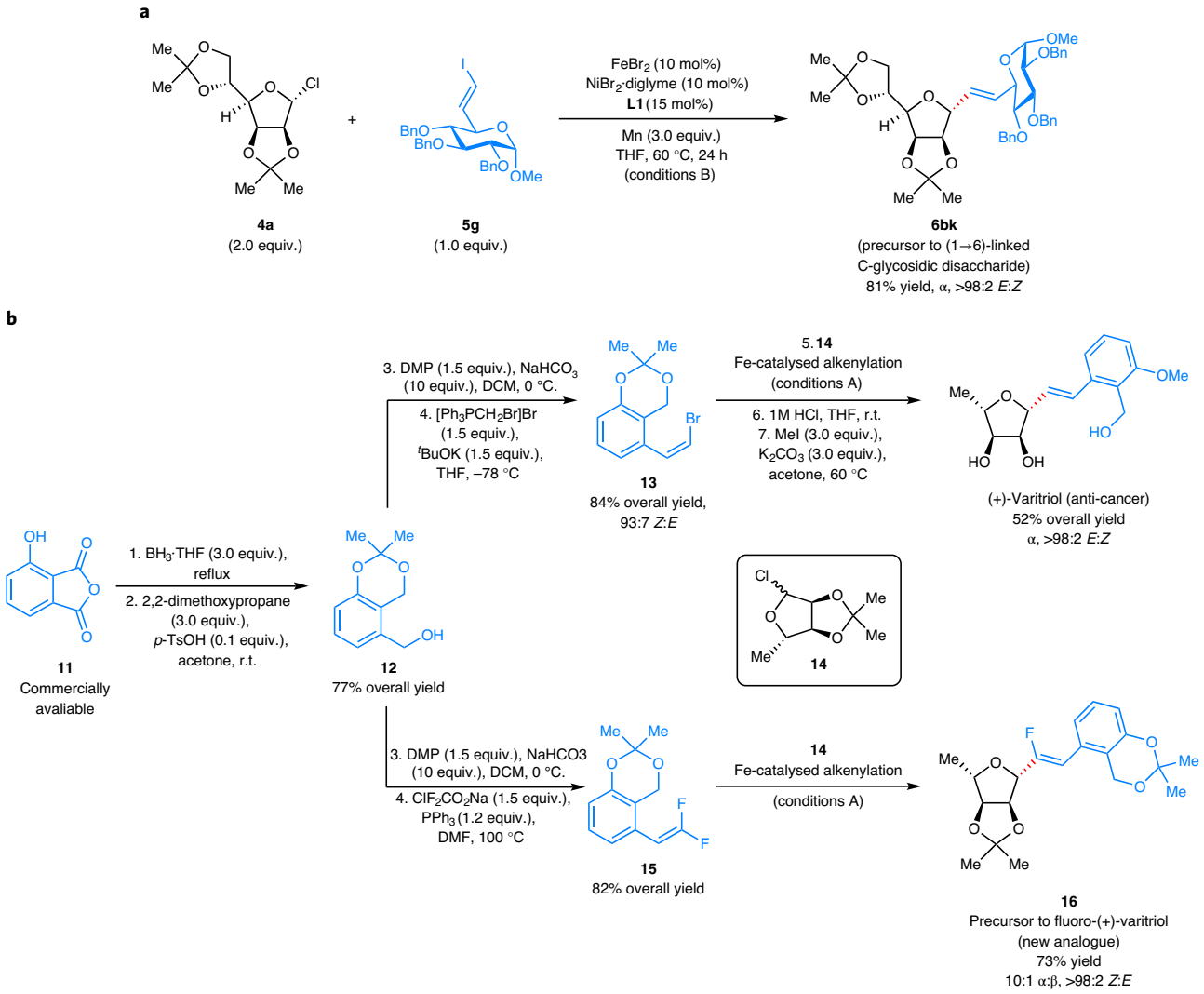

Fig. 5 | Access to biologically relevant carbohydrates and analogues. a, The reductive cross-coupling strategy is amenable to the synthesis of (1→6)-linked pseudodisaccharide building blocks. **b**, The anticancer agent (+)-varitriol and its fluorinated derivative can be readily obtained using Fe-catalysed reductive cross-coupling as the key step. The α:β anomeric ratios and *E*:*Z* ratios were determined by ^{1}H NMR analysis. Yields are for isolated and purified products. *p*-TsOH; *para*-toluenesulfonic acid; DMF, *N*,*N*-dimethylformamide; DCM, dichloromethane.

Substrate scope. We first evaluated the generality of our established conditions by surveying a diverse assortment of functionalized alkenyl halides using **4a** as the glycosyl donor (Table 1). Using conditions A, disubstituted bromoalkenes that bore electron-rich, neutral or electron-deficient arenes served as effective substrates to afford the desired C-alkenyl glycosides **6e**–**6m** exclusively as the α-anomer in 60–82% yields and >98% *E* selectivity. The configuration of **6f** was ascertained by X-ray crystallographic analysis. With a *Z*-alkenyl bromide, conditions B were employed to preserve the olefin geometry, and the desired product *Z*-**6n** could be generated in 6.6:1 α:β ratio. As many medicinally important C-alkenyl glycosides carry an *E* olefin appendage[32], our protocol offers a direct entry to unnatural C-glycosides that bear *Z* alkenes and may possess beneficial properties[72,73]. Products with 1,3-dienes (**6o**) as well as trisubstituted cyclic and acyclic olefins (**6p**–**6r**) were also obtained. Besides haloalkenes, alkenyl triflates (obtained from ketones) are compatible substrates (**6r**), which enable access to a wider set of C-alkenyl glycosides, particularly for scenarios in which preparation of the corresponding alkenyl halide is non-trivial.

α-**6s**, which bears an aliphatic *Z* alkene, can be obtained in 57% yield from the corresponding alkyl-substituted *Z*-alkenyl iodide (<2% product with bromoalkene) under conditions B. It is worth mentioning that 1,1-difluoroalkenes are amenable to cross-coupling[74] to afford products with trisubstituted alkenyl fluorides (**6t**), which further supports our proposed Fe-induced glycosyl radical addition/β-halide elimination mechanism (Fig. 4). By switching to haloalkynes, the desired C-alkynyl glycosides **6u** and **6v** can also be secured (61 and 41% yields, respectively), which underlines the versatility of the catalytic system. Glycosyl chloride donors prepared from a variety of other pyranoses and furanoses participated efficiently in catalytic alkenylation to deliver *E*-**6w**–*E*-**6ai** in 41–81% yields with good control of diastereoselectivity. These include products derived from D-mannopyranose (**6w**–**6y**), D-galactopyranose (**6z**), L-rhamnopyranose (**6aa** and **6ab**), D-arabinofuranose (**6ac**), D-ribofuranose (**6ad**–**6af**), D-lyxofuranose (**6ag**) and D-gulofuranose (**6ah** and **6ai**).

Besides alkenyl and alkynyl halides, transformations with aromatic and heteroaromatic electrophiles (chlorides and triflates) were similarly efficient and diastereoselective (Table 2). With the exception of **6aj**, which could be formed in 62% yield using a single Fe catalytic system, conditions B were found to be applicable for most cases. In the presence of **4a** as the glycosyl donor, C-glycosides that

contained various monocyclic and bicyclic heteroarenes on the anomeric carbon were afforded in 44–70% yields solely as α-anomers. Examples of heteroaryl moieties that could be installed include thiazole (**6aq**), benzothiazoles (**6am–6ap**) and benzimidazoles (**6ak** and **6al**), as well as six-membered nitrogen-rich heterocycles, such as pyrimidines (**6as–6au** and **6ay**), pyrazine (**6av**) and pyridines (**6aw** and **6ax**). The reactions to generate **6aj**, **6ao** and **6aq** proceeded chemoselectively at the presumably more activated C(sp^2)–Cl site adjacent to the electron-withdrawing heteroatom(s). Of particular note, the synthesis of **6aw** highlighted that cross-coupling was more efficient with an organochloride (64% yield compared with a yield of ~15% for the corresponding bromide) and could occur at positions distant from the electrophilic nitrogen. This could be attributed to the greater reactivity[51] of bromoheteroarenes which inadvertently leads to a shorter catalyst lifetime.

Organotriflates (obtained from phenols) were viable substrates under the established conditions and furnished α-**6ax–6ba** in 64–91% yields. Both heteroaryl- (**6ax and 6ay**) and non-heteroaryl-substituted (**6az and 6ba**) products could be formed. Access to **6ba** (derived from female sex hormone oestrone) shows that our system is compatible with complex bioactive compounds. It is worth noting that the preparation of **6ba** by previous protocols using arylzinc compounds[25] may pose complications in the reagent synthesis, given the susceptibility of electrophilic ketones towards organozinc nucleophiles[75]. Different classes of glycosyl chlorides prepared from D-mannopyranose (**6bb**), L-rhamnopyranose (**6bc and 6bd**), D-ribofuranose (**6be** and **6bf**), D-lyxofuranose (**6bg**), D-gulofuranose (**6bh** and **6bi**) and D-arabinofuranose (**6bj**) underwent catalytic heteroarylation to give the expected stereodefined C-glycosides in 39–81% yields. Although the reaction that led to C-riboside **6bf** was less stereoselective (1:2.6 α:β ratio), the desired β-anomer was easily separated by conventional silica gel purification and isolated in 51% yield. β-**6bf** could be elaborated to C-nucleoside **3**, which exhibits potent anti-influenza activity[76].

Synthetic applications. To showcase the utility of our developed catalytic regime, the formal synthesis of a (1→6)-linked C-glycosidic disaccharide, a stable mimic of the naturally occurring *O*-disaccharide[77], was achieved by reacting **1a** with the glucose-derived alkenyl iodide **5g** under the established Fe–Ni catalytic conditions (Fig. 5a). In the event, C-glycoside α-**6bk** was isolated in 81% yield as a single *E* isomer, which could then be hydrogenated to the saturated disaccharide product. Through this C–C bond-forming approach, other classes of C-oligosaccharides could be expeditiously obtained by merging different combinations of sugar substrates.

In another set of applications (Fig. 5b), commercially available 4-hydroxyisobenzofuran-1,3-dione **11** was first converted into benzyl alcohol **12** (77% overall yield from **11**), which subsequently underwent oxidation with Dess–Martin periodinane (DMP) and Wittig-type olefination to afford bromoalkene **13** (93:7 *Z*:*E*) in 84% yield over two steps. This sets the stage for the ensuing Fe-catalysed reductive coupling reaction with glycosyl chloride **14** to give the expected C-alkenyl glycoside (64% yield, 7.8:1 α:β ratio, >98% *E* selectivity). After acetal deprotection and methylation, the anticancer agent (+)-varitriol was isolated as a single α-anomer (52% yield over three steps from **13**). Synthesis of the monofluoro variant of (+)-varitriol was accomplished by coupling **14** with 1,1-difluoroalkene **15**, which could be easily secured from the same alcohol intermediate **12** through a two-step oxidation–difluoroalkenylation sequence. The desired product *Z*-**16**, a precursor to fluoro-(+)-varitriol, was furnished in 73% yield and 10:1 α:β ratio. To summarize, the present catalytic regime provides a convenient avenue to access biologically active C-glycosides and related synthetic analogues.

Conclusions

We have demonstrated that a simple iron-based catalyst is capable of activating glycosyl chlorides under mild reductive conditions to furnish reactive glycosyl radical species, which can be exploited for stereoselective C–C bond-forming transformations. By merging with stable halide or pseudohalide electrophiles through a single Fe or dual Fe–Ni catalytic manifold, a wide range of C-glycosides that bear a functionalized alkenyl, alkynyl or aromatic anomeric group can be accessed in a straightforward manner. The method is applicable to complex bioactive molecule synthesis and offers a general platform to generate drug analogues for compound library screening. We expect the present protocol to find broad utility in carbohydrate research and advance efforts towards the development of catalytic organoiron chemistry for sustainable organic synthesis[78].

Methods

General procedure for cross-coupling with conditions A. In a N_2-filled glove box, an oven-dried 4 ml vial equipped with a magnetic stir bar was charged with $FeBr_2$ (10–20 mol%), Mn (3.0 equiv.), glycosyl chloride (2.0 equiv.) and the organohalide (0.1 mmol, 1.0 equiv.) in THF (0.4 ml). The 4 ml vial was sealed with a polytetrafluoroethylene cap and removed from the glove box. The reaction mixture was allowed to stir at r.t. for 24–48 h. The reaction mixture was concentrated in vacuo and the resulting residue was purified by silica gel flash chromatography to give the desired product.

General procedure for cross-coupling with conditions B. In a N_2-filled glove box, an oven-dried 4 ml vial equipped with a magnetic stir bar was charged with $FeBr_2$ (10–20 mol%), Mn (3.0 equiv.), $NiBr_2$·diglyme (10 mol%), **L1** (15 mol%), glycosyl chloride (2.0 equiv.) and the organohalide (0.1 mmol, 1.0 equiv.) in THF (0.4 ml). The 4 ml vial was sealed with a polytetrafluoroethylene cap and removed from the glove box. The reaction mixture was allowed to stir at r.t. for 24 h. The reaction mixture was concentrated in vacuo and the resulting residue was purified by silica gel flash chromatography to give the desired product.

Data availability

All data supporting the findings of this study are available within the Article and its Supplementary Information. Crystallographic data for the structure (**6f**) reported in this Article have been deposited at the Cambridge Crystallographic Data Centre, under deposition number CCDC 2056391. Copies of the data can be obtained free of charge via https://www.ccdc.cam.ac.uk/structures/.

Received: 31 July 2021; Accepted: 4 January 2022;
Published online: 17 February 2022

References

1. Han, F.-S. Transition-metal-catalyzed Suzuki–Miyaura cross-coupling reactions: a remarkable advance from palladium to nickel catalysts. *Chem. Soc. Rev.* **42**, 5270–5298 (2013).
2. Biffis, A., Centomo, P., Del Zotto, A. & Zecca, M. Pd metal catalysts for cross-couplings and related reactions in the 21st century: a critical review. *Chem. Rev.* **118**, 2249–2295 (2018).
3. Magano, J. & Dunetz, J. R. Large-scale applications of transition metal-catalyzed couplings for the synthesis of pharmaceuticals. *Chem. Rev.* **111**, 2177–2250 (2011).
4. Nicolaou, K. C., Bulger, P. G. & Sarlah, D. Palladium-catalyzed cross-coupling reactions in total synthesis. *Angew. Chem. Int. Ed.* **44**, 4442–4489 (2005).
5. Corbet, J. P. & Mignani, G. Selected patented cross-coupling reaction technologies. *Chem. Rev.* **106**, 2651–2710 (2006).
6. Buono, F., Nguyen, T., Qu, B., Wu, H. & Haddad, N. Recent advances in nonprecious metal catalysis. *Org. Process Res. Dev.* **25**, 1471–1495 (2021).
7. Fürstner, A., Leitner, A., Méndez, M. & Krause, H. Iron-catalyzed cross-coupling reactions. *J. Am. Chem. Soc.* **124**, 13856–13863 (2002).
8. Campeau, L. C. & Hazari, N. Cross-coupling and related reactions: connecting past success to the development of new reactions for the future. *Organometallics* **38**, 3–35 (2019).
9. Tasker, S. Z., Standley, E. A. & Jamison, T. F. Recent advances in homogeneous nickel catalysis. *Nature* **509**, 299–309 (2014).
10. Holland, P. L. Reaction: opportunities for sustainable catalysts. *Chem* **2**, 443–447 (2017).
11. Bauer, I. & Knölker, H.-J. Iron catalysis in organic synthesis. *Chem. Rev.* **115**, 3170–3387 (2015).
12. Fürstner, A. Iron catalysis in organic synthesis: a critical assessment of what it takes to make this base metal a multitasking champion. *ACS Cent. Sci.* **2**, 778–789 (2016).

13. Rana, S., Biswas, J. P., Paul, S., Paik, A. & Maiti, D. Organic synthesis with the most abundant transition metal—iron: from rust to multitasking catalysts. *Chem. Soc. Rev.* **50**, 243–472 (2021).
14. Piontek, A., Bisz, E. & Szostak, M. Iron-catalyzed cross-couplings in the synthesis of pharmaceuticals: in pursuit of sustainability. *Angew. Chem. Int. Ed.* **57**, 11116–11128 (2018).
15. Mako, T. L. & Byers, J. A. Recent advances in iron-catalysed cross coupling reactions and their mechanistic underpinning. *Inorg. Chem. Front.* **3**, 766–790 (2016).
16. Zweig, J. E., Kim, D. E. & Newhouse, T. R. Methods utilizing first-row transition metals in natural product total synthesis. *Chem. Rev.* **117**, 11680–11752 (2017).
17. Neidig, M. L. et al. Development and evolution of mechanistic understanding in iron-catalyzed cross-coupling. *Acc. Chem. Res.* **52**, 140–150 (2019).
18. Sears, J. D., Neate, P. G. N. & Neidig, M. L. Intermediates and mechanism in iron-catalyzed cross-coupling. *J. Am. Chem. Soc.* **140**, 11872–11883 (2018).
19. Ye, Y., Chen, H.-F., Yao, K. & Gong, H.-G. Iron-catalyzed reductive vinylation of tertiary alkyl oxalates with activated vinyl halides. *Org. Lett.* **22**, 2070–2075 (2020).
20. Everson, D. A. & Weix, D. J. Cross-electrophile coupling: principles of reactivity and selectivity. *J. Org. Chem.* **79**, 4793–4798 (2014).
21. Beau, J.-M. & Gallagher, T. in *Glycoscience Synthesis of Substrate Analogs and Mimetics* (eds Driguez, H. & Thiem, J.) 1–54 (Springer, 1998).
22. Nicotra, F. Synthesis of C-glycosides of biological interest. *Top. Curr. Chem.* **187**, 55–83 (1997).
23. Yuan, X. J. & Linhardt, R. J. Recent advances in stereoselective C-glycoside synthesis. *Tetrahedron* **54**, 9912–9959 (1998).
24. Postema, M. H. D. Recent developments in the synthesis of C-glycosides. *Tetrahedron* **48**, 8545–8599 (1992).
25. Adak, L. et al. Synthesis of aryl C-glycosides via iron-catalyzed cross coupling of halosugars: stereoselective anomeric arylation of glycosyl radicals. *J. Am. Chem. Soc.* **139**, 10693–10701 (2017).
26. Lo, J.-C., Gui, J., Yabe, Y., Pan, C. M. & Baran, P. S. Functionalized olefin cross-coupling to construct carbon–carbon bonds. *Nature* **516**, 343–348 (2014).
27. Tardieu, D. et al. Stereoselective synthesis of *C,C*-glycosides from exo-glycals enabled by iron-mediated hydrogen atom transfer. *Org. Lett.* **18**, 7262–7267 (2019).
28. Štambaský, J., Hocek, M. & Kočovský, P. C-nucleosides: synthetic strategies and biological applications. *Chem. Rev.* **109**, 6729–6764 (2009).
29. Granier, T. & Vasella, A. Synthesis and evaluation as glycosidase inhibitors of 1H-imidazol-2-yl C-glycopyranosides. *Helv. Chim. Acta* **78**, 1738–1746 (1995).
30. Temburnikar, K. & Seley-Radtke, K. L. Recent advances in synthetic approaches for medicinal chemistry of *C*-nucleosides. *Beilstein J. Org. Chem.* **14**, 772–785 (2018).
31. Kitamura, K., Ando, Y., Matsumoto, T. & Suzuki, K. Total synthesis of aryl C-glycoside natural products: Strategies and tactics. *Chem. Rev.* **118**, 1495–1598 (2018).
32. Yang, Y. & Yu, B. Recent advances in the chemical synthesis of C-glycosides. *Chem. Rev.* **117**, 12281–12356 (2017).
33. Bokor, É. et al. C-glycopyranosyl arenes and hetarenes: synthetic methods and bioactivity focused on antidiabetic potential. *Chem. Rev.* **117**, 1687–1764 (2017).
34. Guisán-Ceinos, M., Tato, F., Buñuel, E., Calle, P. & Cárdenas, D. J. Fe-catalysed Kumada-type alkyl–alkyl cross-coupling. Evidence for the intermediacy of Fe(I) complexes. *Chem. Sci.* **4**, 1098–1104 (2013).
35. Adams, C. J. et al. Iron(I) in Negishi cross-coupling reactions. *J. Am. Chem. Soc.* **134**, 10333–10336 (2012).
36. Hill, D. H., Parvez, M. A. & Sen, A. Mechanistic aspects of the reaction of anionic iron(0)–olefin complexes with organic halides. Detection and characterization of paramagnetic organometallic intermediates. *J. Am. Chem. Soc.* **116**, 2889–2901 (1994).
37. Cheung, C.-W., Zhurkin, F. E. & Hu, X.-L. *Z*-Selective olefin synthesis via iron-catalyzed reductive coupling of alkyl halides with terminal arylalkynes. *J. Am. Chem. Soc.* **137**, 4932–4935 (2015).
38. Fleischauer, V. E., Muñoz, S. B. III, Neate, P. G. N., Brennessel, W. W. & Neidig, M. M. NHC and nucleophile chelation effects on reactive iron(II) species in alkyl–alkyl cross-coupling. *Chem. Sci.* **9**, 1878–1891 (2018).
39. Rummelt, S. M., Peterson, P. O., Zhong, H. Y. & Chirik, P. J. Oxidative addition of aryl and alkyl halides to a reduced iron pincer complex. *J. Am. Chem. Soc.* **143**, 5928–5936 (2021).
40. Liu, J., Ye, Y., Sessler, J. L. & Gong, H. Cross-electrophile couplings of activated and sterically hindered halides and alcohol derivatives. *Acc. Chem. Res.* **53**, 1833–1845 (2020).
41. Xu, L.-Y., Fan, N.-L. & Hu, X.-G. Recent development in the synthesis of C-glycosides involving glycosyl radicals. *Org. Biomol. Chem.* **18**, 5095–5109 (2020).
42. Harris, J. D., Oelkers, A. B. & Tyler, D. R. The solvent cage effect: is there a spin barrier to recombination of transition metal radicals? *J. Am. Chem. Soc.* **129**, 6255–6262 (2007).
43. Barry, J. T., Berg, D. J. & Tyler, D. R. Radical cage effects: the prediction of radical cage pair recombination efficiencies using microviscosity across a range of solvent types. *J. Am. Chem. Soc.* **139**, 14399–14405 (2017).
44. Yu, X.-L., Zheng, H.-L., Zhao, H.-N., Lee, B. C. & Koh, M. J. Iron-catalyzed regioselective alkenylboration of olefins. *Angew. Chem. Int. Ed.* **60**, 2104–2109 (2021).
45. Wei, Y.-L., Ben-Zvi, B. & Diao, T.-N. Diastereoselective synthesis of aryl *C*-glycosides from glycosyl esters via C–O bond homolysis. *Angew. Chem. Int. Ed.* **60**, 9433–9438 (2021).
46. Liu, J.-D. & Gong, H. Stereoselective preparation of α-C-vinyl/aryl glycosides via nickel-catalyzed reductive coupling of glycosyl halides with vinyl and aryl halides. *Org. Lett.* **20**, 7991–7995 (2018).
47. Dumoulin, A., Matsui, J. K., Gutiérrez-Bonet, Á. & Molander, G. A. Synthesis of non-classical arylated C-saccharides through nickel/photoredox dual catalysis. *Angew. Chem. Int. Ed.* **57**, 6614–6618 (2018).
48. Mou, Z.-D., Wang, J.-X. & Niu, D. W. Stereoselective preparation of C-aryl glycosides via visible-light-induced nickel-catalyzed reductive cross-coupling of glycosyl chlorides and aryl bromides. *Adv. Synth. Catal.* **363**, 3025–3029 (2021).
49. Kim, S., Goldfogel, M. J., Gilbert, M. M. & Weix, D. J. Nickel-catalyzed cross-electrophile coupling of aryl chlorides with primary alkyl chlorides. *J. Am. Chem. Soc.* **142**, 9902–9907 (2020).
50. Olivares, A. M. & Weix, D. J. Multimetallic Ni- and Pd-catalyzed cross-electrophile coupling to form highly substituted 1,3-dienes. *J. Am. Chem. Soc.* **140**, 2446–2449 (2018).
51. Huang, L., Ackerman, L. K. G., Kang, K., Parsons, A. M. & Weix, D. J. LiCl-accelerated multimetallic cross-coupling of aryl chlorides with aryl triflates. *J. Am. Chem. Soc.* **141**, 10978–10983 (2019).
52. Kang, K., Huang, L. & Weix, D. J. Sulfonate versus sulfonate: nickel and palladium multimetallic cross-electrophile coupling of aryl triflates with aryl tosylates. *J. Am. Chem. Soc.* **142**, 10634–10640 (2020).
53. Li, M. et al. Visible-light-induced Pd-catalyzed radical strategy for constructing C-vinyl glycosides. *Org. Lett.* **22**, 6288–6293 (2020).
54. Ghosh, S. & Pradhan, T. K. Stereoselective total synthesis of (+)-varitriol, (−)-varitriol, 5′-*epi*-(+)-varitriol, and 4′-*epi*-(−)-varitriol from D-mannitol. *J. Org. Chem.* **75**, 2107–2110 (2010).
55. Sánchez-Eleuterio, A., García-Santos, W. H., Díaz-Salazar, H., Hernández-Rodríguez, M. & Cordero-Vargas, A. Stereocontrolled nucleophilic addition to five-membered oxocarbenium ions directed by the protecting groups. Application to the total synthesis of (+)-varitriol and of two diastereoisomers thereof. *J. Org. Chem.* **82**, 8464–8475 (2017).
56. Koh, M. J., Nguyen, T. T., Zhang, H.-M., Schrock, R. R. & Hoveyda, A. H. Direct synthesis of *Z*-alkenyl halides through catalytic cross-metathesis. *Nature* **531**, 459–465 (2016).
57. Gillis, E. P., Eastman, K. J., Hill, M. D., Donnelly, D. J. & Meanwell, N. A. Applications of fluorine in medicinal chemistry. *J. Med. Chem.* **58**, 8315–8359 (2015).
58. Wang, Q. Q. et al. Palladium-catalysed C–H glycosylation for synthesis of C-aryl glycosides. *Nat. Catal.* **2**, 793–800 (2019).
59. Düfert, M. A., Billingsley, K. L. & Buchwald, S. L. Suzuki–Miyaura cross-coupling of unprotected, nitrogen-rich heterocycles: substrate scope and mechanistic investigation. *J. Am. Chem. Soc.* **135**, 12877–12885 (2013).
60. Zhu, M.-X. & Messaoudi, S. Diastereoselective decarboxylative alkynylation of anomeric carboxylic acids using Cu/photoredox dual catalysis. *ACS Catal.* **11**, 6334–6342 (2021).
61. Kusunuru, A. K., Tatina, M., Yousuf, S. K. & Mukherjee, D. Copper mediated stereoselective synthesis of C-glycosides from unactivated alkynes. *Commun. Chem.* **49**, 10154–10156 (2013).
62. Wilkinson, B. L., Bornaghi, L. F., Poulsen, S.-A. & Houston, T. A. Synthetic utility of glycosyl triazoles in carbohydrate chemistry. *Tetrahedron.* **62**, 8115–8125 (2006).
63. Hatakeyama, T., Hashimoto, S., Ishizuka, K. & Nakamura, M. Highly selective biaryl cross-coupling reactions between aryl halides and aryl Grignard reagents: a new catalyst combination of N-heterocyclic carbenes and iron, cobalt, and nickel fluorides. *J. Am. Chem. Soc.* **131**, 11949–11963 (2009).
64. Prier, C. K. & MacMillan, D. W. Amine α-heteroarylation via photoredox catalysis: a homolytic aromatic substitution pathway. *Chem. Sci.* **5**, 4173–4178 (2014).
65. Masuda, K., Nagatomo, M. & Inoue, M. Direct assembly of multiply oxygenated carbon chains by decarbonylative radical–radical coupling reactions. *Nat. Chem.* **9**, 207–212 (2016).
66. Igarashi, K. The Koenigs–Knorr reaction. *Adv. Carbohydr. Chem. Biochem.* **34**, 243–283 (1977).
67. Li, M. et al. Transition-metal-free chemo- and regioselective vinylation of azaallyls. *Nat. Chem.* **9**, 997–1004 (2017).

68. Yu, Y., Smith, J. M., Flaschenriem, C. J. & Holland, P. L. Binding affinity of alkynes and alkenes to low-coordinate iron. *Inorg. Chem.* **45**, 5742–5751 (2006).
69. Weidauer, M., Irran, E., Someya, C. I., Haberberger, M. & Enthaler, S. Nickel-catalyzed hydrodehalogenation of aryl halides. *J. Organomet. Chem.* **729**, 53–59 (2013).
70. Manzoor, A., Wienefeld, P., Baird, M. C. & Budzelaar, P. H. M. Catalysis of cross-coupling and homocoupling reactions of aryl halides utilizing Ni(0), Ni(I), and Ni(II) precursors; Ni(0) compounds as the probable catalytic species but Ni(I) compounds as intermediates and products. *Organometallics* **36**, 3508–3519 (2017).
71. Zhu, F. & Walczak, M. A. Stereochemistry of transition metal complexes controlled by the metallo-anomeric effect. *J. Am. Chem. Soc.* **142**, 15127–15136 (2020).
72. Dugave, C. & Demange, L. *cis–trans* isomerization of organic molecules and biomolecules: implications and applications. *Chem. Rev.* **103**, 2475–2532 (2003).
73. Gaspari, R., Prota, A. E., Bargsten, K., Cavalli, A. & Steinmetz, M. O. Structural basis of *cis*- and *trans*-combretastatin binding to tubulin. *Chem* **2**, 102–113 (2017).
74. Lu, X. et al. Nickel-catalyzed defluorinative reductive cross-coupling of *gem*-difluoroalkenes with unactivated secondary and tertiary alkyl halides. *J. Am. Chem. Soc.* **139**, 12632–12637 (2017).
75. Pu, L. & Yu, H.-B. Catalytic asymmetric organozinc additions to carbonyl compounds. *Chem. Rev.* **101**, 757–824 (2001).
76. Wang, G.-Y. et al. Synthesis and anti-influenza activity of pyridine, pyridazine, and pyrimidine C-nucleosides as favipiravir (T-705) analogues. *J. Med. Chem.* **59**, 4611–4624 (2016).
77. Koester, D. C., Kriemen, E. & Werz, D. B. Flexible synthesis of 2-deoxy-C-glycosides and (1→2)-, (1→3)-, and (1→4)-linked C-glycosides. *Angew. Chem. Int. Ed.* **52**, 2985–2989 (2013).
78. Enthaler, S., Junge, K. & Beller, M. Sustainable metal catalysis with iron: from rust to a rising star? *Angew. Chem. Int. Ed.* **47**, 3317–3321 (2008).

Acknowledgements

This research was supported by the Research Scholarship Block from the Ministry of Education, Singapore: C-143-000-207-532, C-141-000-777-532 and C-141-000-333-532 (M.J.K.), and NSFC-21725204 (G.C.). We thank G. K. Tan (National University of Singapore) for X-ray crystallographic analysis. We thank X.-X. Wang and X. Lu (University of Science and Technology of China) for assistance in preparing samples for the electron paramagnetic resonance experiments.

Author contributions

Q.W., Q.S., Y.J. and H.Z. developed the catalytic method. L.Y. and C.T. carried out the electron paramagnetic resonance experiments. M.J.K. and G.C. directed the investigations. M.J.K. wrote the manuscript with revisions provided by the other authors.

Competing interests

The authors declare no competing interests.

Additional information

Supplementary information The online version contains supplementary material available at https://doi.org/10.1038/s44160-022-00024-5.

Correspondence and requests for materials should be addressed to Gong Chen or Ming Joo Koh.

Peer review information *Nature Synthesis* thanks the anonymous reviewers for their contribution to the peer review of this work. Thomas West was the primary editor on this article and managed its editorial process and peer review in collaboration with the rest of the editorial team.

Reprints and permissions information is available at www.nature.com/reprints.

Publisher's note Springer Nature remains neutral with regard to jurisdictional claims in published maps and institutional affiliations.

© The Author(s), under exclusive licence to Springer Nature Limited 2022